the difference Fourier had a height of 0.70 e/Å^3 (estimated error based on $\Delta F = 0.20$).

Acknowledgment. We gratefully acknowledge support from the Petroleum Research Fund, administered by the American Chemical Society, the Jesse H. Jones Foundation, and the University of Notre Dame for financial aid.

Supplementary Material Available: An ORTEP plot and full tables of data collection parameters, bond lengths, bond angles, positional parameters for hydrogen atoms, and thermal parameters for all atoms of complex **5** (14 pages); a listing of calculated and experimental structure factors (10 pages). Ordering information is given on any current masthead page.

---

(34) Reference 32, Table 2.3.1.

Contribution from the Department of Chemistry,
University of South Carolina, Columbia, South Carolina 29208

Cluster Synthesis. 36. New Platinum–Ruthenium and Platinum–Osmium Carbonyl Cluster Complexes from the Reactions of the Complexes $Pt_2M_4(CO)_{18}$ (M = Ru, Os) with Cycloocta-1,5-diene in the Presence of UV Irradiation

Richard D. Adams,* Michael S. Alexander, Isam Arafa, and Wengan Wu

Received May 15, 1991

The reactions of $Pt_2M_4(CO)_{18}$ (**1a**, M = Ru; **1b**, M = Os) with cycloocta-1,5-diene (COD) in the presence of UV irradiation were studied. The reaction of **1a** yielded the new mixed-metal cluster compounds $PtRu_4(CO)_{12}(\mu_4\text{-}CO)(COD)$ (**2**) (11%) and $Pt_4Ru_5(CO)_{20}(COD)$ (**3**) (16%). Compounds **2** and **3** were characterized by IR, ^{1}H NMR, and single-crystal X-ray diffraction analyses. The cluster of **2** consists of a butterfly tetrahedron of four ruthenium atoms that is capped on one of the triangular faces by a Pt(COD) group. A μ_4-η^2-CO ligand lies in the fold of the butterfly. The cluster of compound **3** consists of nine metal atoms and can be described as combination of a Pt_3Ru_3 octahedron fused to a Pt_3Ru_2 square pyramid with a common Pt_3 face and a Pt(COD) capping group on the Ru_3 face of the octahedron. The reaction of **1b** yielded the hexanuclear products $Pt_2Os_4(CO)_{17}$ (**5**) (29%) and $Pt_2Os_4(CO)_{15}(COD)$ (**6**) (25%) and small amounts of the known hexanuclear compounds $Pt_2Os_4(CO)_{12}(COD)_2$ (**8**) (6%) and $PtOs_2(CO)_8(COD)$ (**4**) (7%). Compound **6** was characterized crystallographically. The cluster of **6** exhibits the well-known triangle of triangles "raft" structure with a Pt(COD) grouping on one of the outer triangles and one Pt(CO) group in the inner triangle. Compound **5** is believed to possess a structure similar to **6** but with two CO ligands in the place of the COD ligand. Cyclic voltammetric measurements on compound **5** showed the presence of two reversible one-electron reductions at $E_{1/2} = -0.57$ and -0.84 V. Compound **6** shows two quasireversible one-electron reductions at $E_{1/2} = -0.67$ and -0.93 V. Crystal data: for **2**, space group = $P\bar{1}$, $a = 10.544$ (1) Å, $b = 17.064$ (4) Å, $c = 8.847$ (2) Å, $\alpha = 104.31$ (2)°, $\beta = 98.36$ (2)°, $\gamma = 74.27$ (2)°, $Z = 2$, 2355 reflections, $R = 0.028$; for **3**, space group = $C2/c$, $a = 26.361$ (4) Å, $b = 9.474$ (4) Å, $c = 31.211$ (4) Å, $\beta = 94.85$ (1)°, $Z = 8$, 3769 reflections, $R = 0.026$; for **6**, space group = $Pbca$, $a = 14.781$ (3) Å, $b = 35.83$ (2) Å, $c = 11.548$ (2) Å, $Z = 8$, 2047 reflections, $R = 0.035$.

Introduction

Interest in the chemistry of heteronuclear cluster complexes containing platinum[1] has been stimulated by the importance of heterobimetallic "clusters" containing platinum as catalysts in the petroleum-refining process.[2] We have recently found that the reactions of $Pt(COD)_2$ (COD = cycloocta-1,5-diene) with the pentacarbonyl complexes of iron, ruthenium, and osmium readily yield new mixed-metal carbonyl cluster complexes containing platinum.[3-5] The compounds $Pt_2M_4(CO)_{18}$ (**1a**, M = Ru;[4] **1b**, M = Os[5,6]) have been obtained by this method. These molecules have been shown to have a puckered ladderlike structure consisting of two mutually bonded Pt(CO) groupings between pairs of mutually bonded $M(CO)_4$ groups. The molecules can be split in two by reaction with dppe[4] or CO at 50 atm/25 °C[6] (eq 1). Thermal decarbonylation of **1b** in the presence of COD has yielded the new complexes $Pt_2Os_4(CO)_{12}(COD)_2$ and $Pt_2Os_4(CO)_{11}(COD)_2$.[7] The latter is electronically unsaturated and has been shown to engage in facile addition of selected small molecules.[7] In a continuation of our studies of the compounds **1**, we have now investigated the nature of their reactions with COD in the presence of UV irradiation. Details of this study are described in this report.

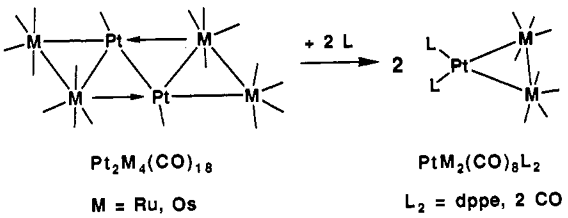

(1)

Experimental Section

General Procedures. Reactions were performed under a dry nitrogen atmosphere. Reagent grade solvents were dried over sodium and deoxygenated by purging with nitrogen prior to use. $Pt_2Ru_4(CO)_{18}$[4] and $Pt_2Os_4(CO)_{18}$[5] were prepared by the previously reported procedures. IR spectra were recorded on a Nicolet 5DXB FT-IR spectrophotometer. ^{1}H NMR spectra were recorded on a Bruker AM-300 FT-NMR spectrometer. Elemental microanalyses were performed by Desert Analytics, Tucson, AZ. TLC separations were performed in air by using silica gel (60 Å, F_{254}) on plates (Whatman, 0.25 mm). UV irradiations were performed on reaction solutions contained in Pyrex glassware by using either an 85-W external high-pressure mercury lamp obtained from George Gates & Co. Franklin Square, NY, or a 1000-W medium-pressure mercury lamp.

Reaction of 1a with COD under UV Irradiation. A 25.0-mg sample of $Pt_2Ru_4(CO)_{18}$ (**1a**) (0.0193 mmol) and 250 μL of COD (2.00 mmol) were dissolved in 450 mL of hexane. The solution was irradiated with the medium-pressure UV lamp (1000 W) at 25 °C in the presence of a slow purge of nitrogen for 21 h. The solvent was removed on a rotary evaporator, and the residue was separated from the mixture by TLC on silica gel with a hexane/CH_2Cl_2 (4/1) solvent mixture. This yielded, in

---

[1] (a) Farrugia, L. J. *Adv. Organomet. Chem.* **1990**, *31*, 301. (b) Braunstein, P.; Rose, J. In *Stereochemistry of Organometallic and Inorganic Compounds*; Bernal, I., Ed.; Elsevier: Amsterdam, 1989; Vol. 3.

[2] (a) Biswas, J.; Bickle, G. M.; Gray, P. G.; Do, D. D.; Barbier, *J. Catal. Rev.—Sci. Eng.* **1988**, *30*, 161. (b) Sinfelt, J. H. *Bimetallic Catalysts. Discoveries, Concepts and Applications*; John Wiley & Sons: New York, 1983. (c) Sinfelt, J. H. *Acc. Chem. Res.* **1977**, *10*, 15. (d) Sinfelt, J. H. *Sci. Am.* **1985**, *253*, 90.

[3] Adams, R. D.; Arafa, I.; Chen, G.; Lii, J. C.; Wang, J. G. *Organometallics* **1990**, *9*, 2350.

[4] Adams, R. D.; Chen, G.; Wang, J. G.; Wu, W. *Organometallics* **1990**, *9*, 1339.

[5] Adams, R. D.; Pompeo, M. P.; Wu, W. *Inorg. Chem.* **1991**, *30*, 2899.

[6] Sundberg, P. *J. Chem. Soc., Chem. Commun.* **1987**, 1307.

[7] (a) Adams, R. D.; Wu, W. *Organometallics* **1991**, *10*, 35. (b) Adams, R. D.; Wu, W. *Inorg. Chem.* **1991**, *30*, 3605.

order of elution, 5.3 mg of unreacted **1a**, 2.2 mg of orange-red $PtRu_4(CO)_{12}(\mu_4\text{-}CO)(COD)$ (**2**) (11%), and 3.0 mg of dark brown $Pt_4Ru_5(CO)_{20}(COD)$ (**3**) (16%). IR: for **2** (ν_{CO}, cm^{-1}, in hexane), 2088 (m), 2061 (s), 2040 (vs), 2033 (sh), 2012 (s), 1997 (w), 1979 (vw), 1941 (vw, br), 1928 (vw, br); for **3** (ν_{CO}, cm^{-1}, in CH_2Cl_2), 2090 (m), 2064 (sh), 2051 (vs), 2034 (s) 1991 (vw, br), 1986 (vw, br). ^1H NMR (δ, in $CDCl_3$): for **2**, 5.77 (4 H, $^2J_{Pt-H}$ = 60 Hz), 2.69–2.44 (8 H); for **3** 5.98 (4 H, $^2J_{Pt-H}$ = 58 Hz), 2.80–2.50 (8 H). Anal. Calc (found) for **2**: C, 23.54 (23.77); H, 1.12 (1.06). Calc (found) for **3**: C, 17.21 (16.96); H 0.62 (0.55).

Thermal Reaction of 1a with COD. A 18.1-mg sample of **1a** (0.014 mmol) was allowed to react with 4.0 μL of COD (0.032 mmol) in refluxing hexane (40 mL) for 3 h to yield compound **2** only, 22%.

Reaction of 1b with COD under UV Irradiation. A solution of 14.0 mg of $Pt_2Os_4(CO)_{18}$ (**1b**) (0.0085 mmol) and 0.075 mL of COD (0.60 mmol) in 50 mL of hexane was irradiated by the high-pressure UV lamp (85 W) with a continuous purge of nitrogen for 11 h at 25 °C. The solvent was removed in vacuo, and the residue was separated from the mixture by TLC with a hexane/CH_2Cl_2 (4/1) solvent mixture. This yielded, in order of elution, 1.1 mg of $PtOs_2(CO)_8(COD)$[7] (**4**) (7%), 1.4 mg of unreacted **1b** (11%), 4.0 mg of $Pt_2Os_4(CO)_{17}$ (**5**) (29%), 3.5 mg of gray-green $Pt_2Os_4(CO)_{15}(COD)$ (**6**) (25%), 0.6 mg of unknown brown compound, **7**, and 0.8 mg of $Pt_2Os_4(CO)_{12}(COD)_2$[7] (**8**) (6%). A similar result was obtained when this reaction was carried out with the medium-pressure UV lamp (1000 W). IR (ν_{CO}, cm^{-1}, in hexane): for **6**, 2110 (w), 2078 (s), 2041 (m), 2033 (vs), 2027 (sh), 2015 (m), 1997 (vw), 1987 (w), 1969 (w), 1957 (w); for **7**, 2097 (m), 2068 (s), 2058 (vs), 2038 (m), 2029 (s), 2005 (w), 1988 (w), 1983 (w), 1922 (vw). ^1H NMR (δ, in $CDCl_3$): for **6**, 5.36 (4 H, $^2J_{Pt-H}$ = 64.6 Hz), 2.18 (4 H), 1.96 (4 H). Anal. Calc (found) for **5**: C, 12.55 (12.41); H, 0.00 (0.00). Calc (found) for **6**: C, 16.45 (16.18); H, 0.72 (0.58). The formula of **5** was established from its mass spectrum obtained at 170 °C by direct inlet. The parent ion at m/e = 1628 with the expected isotope distribution for two platinum and four osmium atoms and the ions corresponding to the stepwise loss of 2–17 CO ligands were observed.

Reaction of 6 with CO. An 8.8-mg amount of **6** (0.0054 mmol) was dissolved in 20 mL of hexane, and CO was then allowed to purge through the solution slowly at 25 °C for 5 min. The color of the solution changed from gray-green to brown and then to red during this time. The solvent was removed on a rotary evaporator, and the products were separated from the mixture by TLC. Elution with a hexane/CH_2Cl_2 (4/1) solvent mixture yielded 1.5 mg of yellow $PtOs_2(CO)_{10}$ (**9**) (16%), 3.5 mg of **1b** (40%), and 0.8 mg of **5** (9%).

Reaction of 6 with COD. 1. Thermal Reaction. An 8.0-mg sample of **6** (0.0048 mmol) was allowed to react with 0.10 mL of COD (0.80 mmol) in 15 mL of heptane at 60 °C (water bath) for 1 h. The color of the solution changed from gray-green to red-brown over this period. The solvent was removed on a rotary evaporator, and the residue was separated from the mixture by TLC on silica gel. This yielded 5.0 mg of **8** (62%), 0.3 mg of **4** (3%), 0.5 mg of **1b** (5%), and a trace of **5**.

2. Reaction under UV Irradiation. A solution of 8.0 mg of **6** (0.0048 mmol) and 0.10 mL of COD (0.80 mmol) in 40 mL of hexane was irradiated by the medium-pressure UV lamp (1000 W) at 25 °C for 4 h. This yielded 1.1 mg of **8** (14%) with 3.2 mg of unreacted **6** (40%). Meanwhile, **4**, **1b**, **5**, and $Pt_2Os_4(CO)_{11}(COD)_2$ (**10**) were obtained in trace amounts.

Attempted Reaction of 5 with COD. A 15.0-mg sample of **5** (0.0092 mmol) was allowed to react with 0.10 mL of COD (0.80 mmol) in 80 mL of hexane under UV irradiation (85-W high-pressure UV lamp) with a continuous purge of nitrogen. The reaction was followed by IR spectroscopy, and no change was detected over a period of 20 h. When 20 mg of **5** (0.012 mmol) reacted with 0.20 mL of COD (1.6 mmol) in refluxing heptane for 10 h, 3.0 mg of **8** (14%) was isolated with 13.5 mg of unreacted **5** recovered from the reaction mixture.

Decarbonylation of 1b by UV Irradiation. A solution of 15.0 mg of **1b** in 60 mL of hexane was irradiated by using the 85-W UV lamp for 51 h in the presence of a slow purge of nitrogen through the solution. This yielded 9.5 mg of **5** (64% yield) after workup by TLC.

Attempted Reaction of 5 with CO. A solution of 5.0 mg of **5** in 15 mL of CH_2Cl_2 was purged with CO for 18 h at 25 °C. IR spectroscopy showed no evidence of reaction. The solution was then refluxed for 2 h in the presence of CO, and still no evidence for reaction was found by IR spectroscopy.

Electrochemical Measurements. Cyclic voltammetry measurements were made on a BAS100A electrochemical analyzer. Tetrabutylammonium hexafluorophosphate (0.1 M) was used as the supporting electrolyte. Solutions of the samples in CH_2Cl_2 were prepared under a nitrogen atmosphere, and the electrochemical cell was purged with nitrogen prior to the measurements. The measurements were made at 25 °C by using a platinum electrode with a saturated sodium chloride calomel reference electrode and a scan rate of 100 mV/s. For **5**, 4.2 mg of sample was dissolved in 7 mL of CH_2Cl_2 with 10 μL of H_2O. The voltammogram showed two reversible one-electron redox processes. One centered at $E_{1/2}$ = −0.57 V (i_c/i_a = 1.20, ΔE_p = 84 mV) was assigned to the 0/−1 couple, while the one centered at $E_{1/2}$ = −0.84 V (i_c/i_a = 0.94, ΔE_p = 86 mV) was assigned to the −1/−2 couple. For **6**, 2.8 mg of sample was dissolved in 6 mL of CH_2Cl_2. The cyclic voltammogram of **6** showed two quasireversible one-electron reductions. The one at $E_{1/2}$ = −0.67 V (i_c/i_a = 1.46, ΔE_p = 86 mV) was assigned to the 0/−1 couple. The one at $E_{1/2}$ = −0.93 V (i_c/i_a = 3.73, ΔE_p = 112 mV) was assigned to the −1/−2 couple.

Table I. Crystal Data for Compounds **2**, **3**, and **6**[a]

	2	**3**	**6**
formula	$PtRu_4O_{13}C_{21}H_{12}\cdot 0.5C_6H_6$	$Pt_4Ru_5O_{20}C_{28}H_{12}$	$Pt_2Os_4O_{15}C_{23}H_{12}$
fw	1149.8	1954.1	1679.32
cryst syst	triclinic	monoclinic	orthorhombic
a, Å	10.544 (1)	26.361 (4)	14.781 (3)
b, Å	17.064 (4)	9.474 (4)	35.83 (2)
c, Å	8.847 (2)	31.211 (4)	11.548 (2)
α, deg	104.31 (2)	90.0	90.0
β, deg	98.36 (2)	94.85 (1)	90.0
γ, deg	74.27 (2)	90.0	90.0
V, $Å^3$	1479 (1)	7767 (3)	6116 (4)
space group	$P\bar{1}$ (No. 2)	$C2/c$ (No. 15)	$Pbca$ (No. 61)
Z	2	8	8
ρ_{calc}, g/cm^3	2.49	3.34	3.65
μ(Mo Kα), cm^{-1}	67.8	164.3	258.9
temp, °C	20	20	20
no. of observns ($I > 3\sigma$)	2355	3769	2047
residuals:[b] R, R_w	0.028, 0.030	0.026, 0.027	0.035, 0.034

[a] In this and all subsequent tables, estimated standard deviations in the least significant figure are given in parentheses. [b] $R(F_o) = \sum_{hkl}(||F_o| - |F_c||)/\sum_{hkl}|F_o|$; $R_w(F_o) = [\sum_{hkl}(|F_o| - |F_c|^2)/\sum_{hkl}|F_o|^2]^{1/2}$.

Crystallographic Analysis. Crystals of compound **2** suitable for diffraction analysis were grown by slow evaporation of benzene/heptane (4/1) at 10 °C. Crystals of compound **3** were grown in solution in hexane/CH_2Cl_2 (1/4) solvent by slow evaporation at 10 °C. Crystals of compound **6** were grown by slow evaporation of solvent from ethyl acetate solution at 10 °C. All data crystals were mounted in thin-walled glass capillaries. Diffraction measurements were made on a Rigaku AFC6S fully automated four-circle diffractometer using graphite-monochromatized Mo Kα radiation. Unit cells were determined and refined from 15 randomly selected reflections obtained by using the AFC6 automatic search, center, index, and least-squares routines. Crystal data, data collection parameters, and results of the analyses are listed in Table I. All data processing was performed on a Digital Equipment Corp. VAXstation 3520 computer by using the TEXSAN structure solving program library (version 5.0) obtained from the Molecular Structure Corp., The Woodlands, TX. Neutral-atom scattering factors were calculated by the standard procedures.[8a] Anomalous dispersion corrections were applied to all non-hydrogen atoms.[8b] Lorentz/polarization (Lp) and absorption corrections were applied to the data for each structure. Full-matrix least-squares refinements minimized the function

$$\sum_{hkl} w(|F_o| - |F_c|)^2$$

where

$$w = 1/\sigma(F_o)^2 \qquad \sigma(F_o) = \sigma(F_o^2)/2F_o$$

$$\sigma(F_o^2) = [\sigma(I_{raw})^2 + (0.02I_{net}^2)^2]^{1/2}/Lp$$

Compound **2** crystallized in the triclinic crystal system. The space group $P\bar{1}$ was assumed and confirmed by the successful solution and refinement of the structure. The positions of the metal atoms were obtained by direct methods (MITHRIL). All remaining non-hydrogen atoms were obtained by a series of subsequent difference Fourier syntheses. All non-hydrogen atoms were refined with anisotropic thermal parameters. The positions of the hydrogen atoms on the COD ligands were calculated by using idealized geometries. Their contributions were added to the structure factor calculations, but their positions were not refined. A molecule of benzene from the crystallization solvent was found

---

(8) (a) *International Tables for X-ray Crystallography*; Kynoch Press: Birmingham, England, 1975; Vol. IV, Table 2.2B, pp 99–101. (b) *Ibid.*, Table 2.3.1, pp 149–150.

Table II. Metal and Carbonyl Ligand Positional Parameters and *B*(eq) for **2**

atom	*x*	*y*	*z*	*B*(eq), Å^2
Pt	0.66792 (04)	0.30335 (03)	0.64794 (05)	2.78 (2)
Ru(1)	0.85596 (08)	0.38502 (06)	0.64589 (11)	3.02 (5)
Ru(2)	0.88813 (08)	0.28828 (06)	0.87095 (10)	2.85 (5)
Ru(3)	0.90565 (08)	0.21000 (06)	0.54921 (10)	2.97 (5)
Ru(4)	1.12132 (09)	0.17135 (06)	0.76949 (11)	3.40 (5)
O(10)	1.1353 (07)	0.2852 (04)	0.7220 (08)	3.6 (4)
O(11)	0.6878 (11)	0.5465 (06)	0.8280 (12)	7.2 (6)
O(12)	0.7343 (10)	0.4134 (07)	0.3255 (11)	7.6 (7)
O(13)	1.0803 (10)	0.4654 (07)	0.6390 (14)	8.8 (7)
O(21)	1.0501 (10)	0.3559 (07)	1.1609 (12)	8.4 (7)
O(22)	0.8450 (09)	0.1493 (06)	1.0014 (11)	6.1 (6)
O(23)	0.6461 (08)	0.4165 (05)	1.0118 (09)	5.1 (5)
O(31)	1.1032 (09)	0.1448 (07)	0.2996 (11)	7.2 (6)
O(32)	0.8539 (09)	0.0451 (06)	0.5556 (12)	6.5 (6)
O(33)	0.6928 (09)	0.2312 (06)	0.2793 (10)	6.3 (6)
O(41)	1.2921 (09)	0.1949 (06)	1.0795 (11)	6.1 (6)
O(42)	1.3411 (09)	0.0685 (06)	0.5589 (11)	6.1 (6)
O(43)	1.0729 (09)	0.0157 (06)	0.8257 (11)	6.3 (6)
C(10)	1.0111 (10)	0.2927 (06)	0.7047 (11)	2.3 (6)
C(11)	0.7502 (13)	0.4855 (08)	0.7609 (15)	4.2 (7)
C(12)	0.7778 (12)	0.4035 (08)	0.4457 (16)	4.4 (7)
C(13)	0.9977 (12)	0.4364 (08)	0.6423 (16)	4.9 (8)
C(21)	0.9944 (13)	0.3305 (08)	1.0500 (15)	4.8 (8)
C(22)	0.8611 (11)	0.2015 (07)	0.9534 (13)	3.6 (7)
C(23)	0.7259 (11)	0.3671 (07)	0.9402 (13)	3.4 (6)
C(31)	1.0318 (12)	0.1682 (08)	0.3949 (14)	4.3 (7)
C(32)	0.8735 (11)	0.1053 (08)	0.5535 (14)	4.0 (7)
C(33)	0.7548 (11)	0.2315 (07)	0.3978 (15)	4.1 (7)
C(41)	1.2295 (12)	0.1845 (07)	0.9624 (16)	4.2 (7)
C(42)	1.2580 (13)	0.1060 (08)	0.6385 (16)	4.6 (7)
C(43)	1.0840 (11)	0.0760 (08)	0.8034 (15)	4.4 (7)

cocrystallized with the complex in the final stages of the analysis. It was located on a crystallographic center of symmetry. It was included in the analysis and was satisfactorily refined with isotropic thermal parameters for the carbon atoms.

Compound **3** crystallized in the monoclinic crystal system. The systematic absences in the data were consistent with either space group *Cc* or *C*2/*c*. The latter was selected and confirmed by the successful solution and refinement of the structure. The structure was solved by a combination of direct methods (MITHRIL) and difference Fourier syntheses. All non-hydrogen atoms were refined anisotropically. The positions of the hydrogen atoms on the COD ligand were calculated by using idealized geometries. Their contributions were added to the structure factor calculations, but their positions were not refined.

Compound **6** crystallized in the orthorhombic crystal system. The space group *Pbca* was identified uniquely on the basis of the systematic absences observed in the data. Only the atoms larger than carbon were refined with anisotropic thermal parameters. The positions of all hydrogen atoms were calculated by using idealized geometries. Their contributions were added to the structure factor calculations, but their positions were not refined.

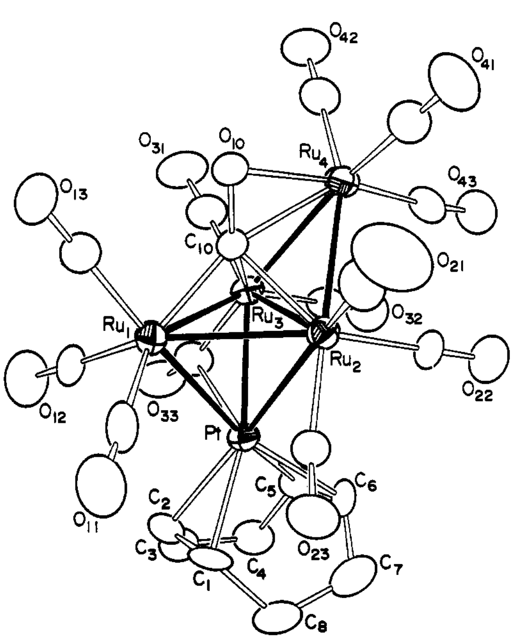

Figure 1. ORTEP diagram of $PtRu_4(CO)_{12}(\mu_4\text{-}CO)(COD)$ (**2**) showing 50% probability thermal ellipsoids.

Table III. Intramolecular Distances (Å) for **2**

Pt–Ru(1)	2.719 (1)	Ru(3)–Ru(4)	2.818 (1)
Pt–Ru(2)	2.819 (1)	Ru(3)–C(10)	2.14 (1)
Pt–Ru(3)	2.714 (1)	Ru(3)–C(31)	1.92 (1)
Pt–C(33)	2.42 (1)	Ru(3)–C(32)	1.92 (1)
Ru(1)–Ru(2)	2.816 (1)	Ru(3)–C(33)	1.94 (1)
Ru(1)–Ru(3)	2.819 (2)	Ru(4)–O(10)	2.132 (7)
Ru(1)–C(10)	2.05 (1)	Ru(4)–C(10)	2.25 (1)
Ru(1)–C(11)	1.91 (1)	Ru(4)–C(41)	1.91 (1)
Ru(1)–C(12)	1.90 (1)	Ru(4)–C(42)	1.91 (1)
Ru(1)–C(13)	1.93 (1)	Ru(4)–C(43)	1.87 (1)
Ru(2)–Ru(3)	2.839 (1)	O(10)–C(10)	1.27 (1)
Ru(2)–Ru(4)	2.816 (1)	C(1)–C(2)	1.36 (2)
Ru(2)–C(10)	2.12 (1)	C(5)–C(6)	1.36 (2)
Ru(2)–C(21)	1.91 (1)	O–C(av)	1.14 (1)
Ru(2)–C(22)	1.90 (1)	Pt–C(23)	2.60 (1)
Ru(2)–C(23)	1.94 (1)		

Table IV. Intramolecular Bond Angles (deg) for **2**

Ru(1)–Pt–Ru(2)	61.09 (3)	Pt–Ru(3)–Ru(2)	60.96 (3)
Ru(1)–Pt–Ru(3)	62.49 (3)	Pt–Ru(3)–Ru(4)	119.99 (4)
Ru(2)–Pt–Ru(3)	61.71 (3)	Ru(1)–Ru(3)–Ru(2)	59.70 (4)
Pt–Ru(1)–Ru(2)	61.20 (3)	Ru(1)–Ru(3)–Ru(4)	97.19 (4)
Pt–Ru(1)–Ru(3)	58.67 (3)	Ru(2)–Ru(3)–Ru(4)	59.71 (3)
Ru(2)–Ru(1)–Ru(3)	60.51 (4)	Ru(2)–Ru(4)–Ru(3)	60.52 (3)
Pt–Ru(2)–Ru(1)	57.71 (3)	Ru(1)–C(10)–O(10)	132.3 (7)
Pt–Ru(2)–Ru(3)	57.34 (3)	Ru(2)–C(10)–O(10)	127.5 (7)
Pt–Ru(2)–Ru(4)	116.47 (4)	Ru(2)–C(23)–O(23)	165 (1)
Ru(1)–Ru(2)–Ru(3)	59.79 (4)	Ru(3)–C(10)–O(10)	127.4 (7)
Ru(1)–Ru(2)–Ru(4)	97.28 (4)	Ru(3)–C(23)–O(23)	160 (1)
Ru(3)–Ru(2)–Ru(4)	59.77 (4)	Ru–C(av)–O	178 (1)
Pt–Ru(3)–Ru(1)	58.84 (3)		

Results

When solutions of $Pt_2Ru_4(CO)_{18}$ (**1a**) (25 mg in 450 mL solvent) and cycloocta-1,5-diene (COD) were exposed to UV irradiation for 21 h, two new platinum–ruthenium carbonyl cluster complexes $PtRu_4(CO)_{12}(\mu_4\text{-}CO)(COD)$ (**2**) and $Pt_4Ru_5(CO)_{20}(COD)$ (**3**) were formed in yields of 11% and 16%, respectively. There were substantial amounts of unreacted **1a**, but longer reaction times did not produce higher yields. When **1a** was allowed to react with COD thermally (97 °C), compound **2** was formed in approximately 22% yield and no **3** was obtained. Compounds **2** and **3** were characterized by a combination of IR, ^1H NMR, and single-crystal X-ray diffraction analyses. An ORTEP diagram of the structure of **2** is shown in Figure 1. Final atomic positional parameters are listed in Table II. Selected interatomic distances and angles are listed in Tables III and IV. The structure of compound **2** consists of a butterfly cluster of four ruthenium atoms that contains a Pt(COD) group capping one triangular face. The platinum–ruthenium bond distances to the Pt(COD) capping group are not unusual but do consist of two short bonds, Pt–Ru(1) = 2.719 (1) Å and Pt–Ru(3) = 2.714 (1) Å, and one long one, Pt–Ru(2) = 2.819 (1) Å.[9] This uneven distribution of the bonds has been observed for other examples of Pt(COD) capping groups on M_3 triangles[9] and may be a consequence of placing a group with 2-fold symmetry on a site with 3-fold symmetry. The most unexpected feature about **2** is the presence of $\mu_4\text{-}\eta^2$-CO ligand that lies in the fold of the Ru_4 butterfly. These ligands have been observed on a number of previous occasions.[10-12] As is typical of this coordination, the CO bond distance is slightly elongated,

---

(9) A listing of Pt–Ru distances for recently published cluster complexes is given in ref 1a.

(10) Horwitz, C. P.; Shriver, D. F. *Adv. Organomet. Chem.* **1984**, *23*, 219.

(11) Adams, R. D.; Babin, J. E.; Tasi, M. *Inorg. Chem.* **1988**, *27*, 2618.

(12) Bailey, P. J.; Duer, M. J.; Johnson, B. F. G.; Lewis, J.; Conole, G.; McPartlin, M.; Powell, H. R.; Anson, C. E. *J. Organomet. Chem.* **1990**, *383*, 441.

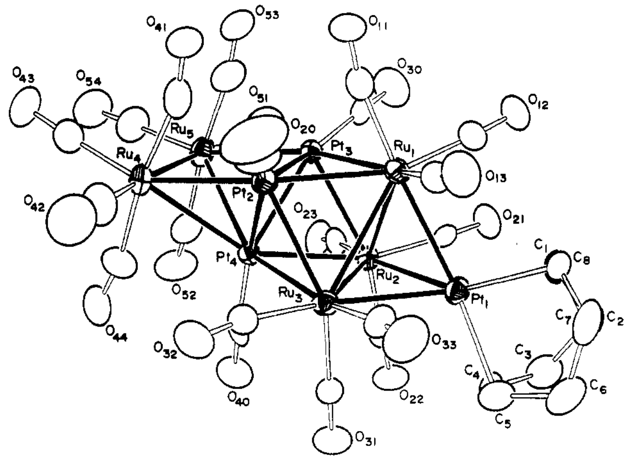

Figure 2. ORTEP diagram of $Pt_4Ru_5(CO)_{20}(COD)$ (**3**) showing 50% probability thermal ellipsoids.

Table V. Positional Parameters and *B*(eq) for **3**

atom	*x*	*y*	*z*	*B*(eq), Å^2
Pt(1)	0.295855 (19)	–0.00383 (05)	0.119593 (13)	2.76 (2)
Pt(2)	0.128617 (20)	0.03281 (05)	0.070451 (13)	2.69 (2)
Pt(3)	0.132641 (19)	–0.16786 (05)	0.130888 (13)	2.41 (2)
Pt(4)	0.128438 (19)	0.10069 (05)	0.152233 (13)	2.48 (2)
Ru(1)	0.21213 (04)	–0.13870 (10)	0.08128 (03)	2.59 (4)
Ru(2)	0.21478 (04)	–0.04993 (10)	0.17586 (02)	2.33 (4)
Ru(3)	0.21210 (04)	0.16838 (10)	0.10997 (03)	2.59 (4)
Ru(4)	0.03552 (05)	0.12887 (12)	0.09410 (03)	3.83 (5)
Ru(5)	0.04074 (04)	–0.08631 (13)	0.16210 (03)	3.77 (5)
O(11)	0.1311 (04)	–0.2996 (11)	0.0245 (03)	5.1 (5)
O(12)	0.2693 (04)	–0.4153 (11)	0.0943 (03)	4.9 (5)
O(13)	0.2630 (04)	–0.0650 (11)	0.0017 (03)	5.1 (5)
O(20)	0.1330 (05)	0.0948 (14)	–0.0234 (03)	8.3 (7)
O(21)	0.2883 (04)	–0.2939 (10)	0.1908 (02)	4.3 (5)
O(22)	0.2780 (04)	0.1192 (10)	0.2416 (03)	5.0 (5)
O(23)	0.1542 (04)	–0.1317 (10)	0.2502 (03)	4.8 (5)
O(30)	0.1570 (05)	–0.4635 (11)	0.1599 (03)	6.8 (7)
O(31)	0.2640 (04)	0.3730 (10)	0.1729 (03)	5.3 (5)
O(32)	0.1491 (05)	0.4059 (11)	0.0680 (03)	6.7 (6)
O(33)	0.2826 (04)	0.2334 (11)	0.0405 (03)	5.7 (6)
O(40)	0.1574 (04)	0.3072 (11)	0.2232 (03)	5.4 (5)
O(41)	0.0284 (04)	–0.1089 (11)	0.0261 (03)	5.5 (6)
O(42)	0.0383 (06)	0.3496 (14)	0.0228 (04)	9.1 (8)
O(43)	–0.0798 (05)	0.1100 (16)	0.0842 (04)	9.9 (9)
O(44)	0.0402 (05)	0.3716 (13)	0.1603 (04)	7.8 (7)
O(51)	0.0560 (06)	–0.3185 (14)	0.2284 (04)	8.9 (8)
O(52)	0.0550 (05)	0.1253 (13)	0.2364 (03)	7.7 (7)
O(53)	0.0265 (04)	–0.3248 (12)	0.0953 (03)	5.8 (6)
O(54)	–0.0735 (05)	–0.0705 (17)	0.1697 (04)	9.4 (9)
C(11)	0.1571 (06)	–0.2332 (15)	0.0477 (04)	3.8 (7)
C(12)	0.2486 (05)	–0.3107 (15)	0.0907 (03)	3.6 (7)
C(13)	0.2461 (05)	–0.0869 (14)	0.0329 (04)	3.5 (6)
C(20)	0.1317 (06)	0.0746 (15)	0.0123 (04)	4.6 (8)
C(21)	0.2627 (05)	–0.1995 (14)	0.1835 (03)	2.6 (6)
C(22)	0.2538 (05)	0.0577 (14)	0.2157 (03)	3.4 (6)
C(23)	0.1755 (05)	–0.1075 (13)	0.2204 (03)	3.1 (6)
C(30)	0.1469 (05)	–0.3505 (15)	0.1483 (04)	3.3 (6)
C(31)	0.2449 (05)	0.2985 (13)	0.1491 (03)	2.9 (6)
C(32)	0.1689 (06)	0.3094 (15)	0.0832 (04)	4.1 (7)
C(33)	0.2589 (05)	0.1957 (14)	0.0683 (04)	3.9 (7)
C(40)	0.1458 (05)	0.2340 (13)	0.1957 (04)	3.5 (6)
C(41)	0.0388 (06)	–0.0254 (16)	0.0524 (04)	4.4 (8)
C(42)	0.0373 (07)	0.2677 (18)	0.0499 (05)	6 (1)
C(43)	–0.0361 (07)	0.1188 (18)	0.0899 (05)	5.7 (9)
C(44)	0.0437 (07)	0.2778 (17)	0.1373 (05)	5.7 (9)
C(51)	0.0523 (07)	–0.2309 (20)	0.2044 (05)	6 (1)
C(52)	0.0535 (06)	0.0571 (17)	0.2061 (05)	5.1 (8)
C(53)	0.0373 (06)	–0.2318 (17)	0.1181 (04)	4.7 (8)
C(54)	–0.0305 (07)	–0.075 (02)	0.1657 (05)	6 (1)

Table VI. Intramolecular Distances (Å) for **3**

Pt(1)–Ru(1)	2.737 (1)	Ru(1)–Ru(2)	3.065 (1)
Pt(1)–Ru(2)	2.911 (1)	Ru(1)–Ru(3)	3.044 (2)
Pt(1)–Ru(3)	2.741 (1)	Ru(1)–C(11)	1.94 (1)
Pt(1)–C(1)	2.18 (1)	Ru(1)–C(12)	1.90 (2)
Pt(1)–C(4)	2.27 (1)	Ru(1)–C(13)	1.88 (1)
Pt(1)–C(5)	2.27 (1)	Ru(2)–Ru(3)	2.913 (1)
Pt(1)–C(8)	2.22 (1)	Ru(2)–C(21)	1.90 (1)
Pt(2)–Pt(3)	2.6740 (8)	Ru(2)–C(22)	1.85 (1)
Pt(2)–Pt(4)	2.6327 (7)	Ru(2)–C(23)	1.88 (1)
Pt(2)–Ru(1)	2.734 (1)	Ru(3)–C(31)	1.89 (1)
Pt(2)–Ru(3)	2.749 (1)	Ru(3)–C(32)	1.90 (1)
Pt(2)–Ru(4)	2.775 (1)	Ru(3)–C(33)	1.88 (1)
Pt(2)–C(20)	1.87 (1)	Ru(4)–Ru(5)	2.938 (2)
Pt(2)–C(41)	2.45 (2)	Ru(4)–C(41)	1.96 (2)
Pt(3)–Pt(4)	2.635 (1)	Ru(4)–C(42)	1.91 (2)
Pt(3)–Ru(1)	2.723 (1)	Ru(4)–C(43)	1.88 (2)
Pt(3)–Ru(2)	2.719 (1)	Ru(4)–C(44)	1.95 (1)
Pt(3)–Ru(5)	2.795 (1)	Ru(5)–C(51)	1.91 (2)
Pt(3)–C(30)	1.84 (1)	Ru(5)–C(52)	1.94 (2)
Pt(3)–C(53)	2.58 (2)	Ru(5)–C(53)	1.94 (2)
Pt(4)–Ru(2)	2.735 (1)	Ru(5)–C(54)	1.89 (2)
Pt(4)–Ru(3)	2.740 (1)	C(1)–C(8)	1.40 (2)
Pt(4)–Ru(4)	2.935 (1)	C(4)–C(5)	1.38 (2)
Pt(4)–Ru(5)	2.949 (1)	O–C(av)	1.14 (1)
Pt(4)–C(40)	1.88 (1)		

Table VII. Intramolecular Bond Angles (deg) for **3**

Pt(3)–Pt(2)–Pt(4)	59.53 (2)	Pt(3)–Pt(4)–Ru(2)	60.82 (3)
Pt(3)–Pt(2)–Ru(1)	60.45 (3)	Pt(3)–Pt(4)–Ru(3)	92.95 (3)
Pt(3)–Pt(2)–Ru(3)	91.90 (3)	Pt(3)–Pt(4)–Ru(4)	88.98 (3)
Pt(3)–Pt(2)–Ru(4)	91.65 (3)	Pt(3)–Pt(4)–Ru(5)	59.76 (3)
Pt(3)–Pt(2)–C(20)	146.6 (4)	Pt(3)–Pt(4)–C(40)	144.8 (3)
Pt(4)–Pt(2)–Ru(1)	95.32 (3)	Ru(2)–Pt(4)–Ru(3)	64.30 (3)
Pt(4)–Pt(2)–Ru(3)	61.17 (3)	Ru(2)–Pt(4)–Ru(4)	147.83 (3)
Pt(4)–Pt(2)–Ru(4)	65.66 (3)	Ru(2)–Pt(4)–Ru(5)	107.48 (4)
Pt(4)–Pt(2)–C(20)	153.5 (4)	Ru(3)–Pt(4)–Ru(4)	110.17 (3)
Ru(1)–Pt(2)–Ru(3)	67.45 (4)	Ru(3)–Pt(4)–Ru(5)	149.41 (3)
Ru(1)–Pt(2)–Ru(4)	152.00 (3)	Ru(4)–Pt(4)–Ru(5)	59.90 (3)
Ru(1)–Pt(2)–C(41)	130.3 (4)	Pt(2)–Ru(1)–Pt(3)	58.68 (3)
Ru(3)–Pt(2)–Ru(4)	114.83 (4)	Pt(3)–Ru(2)–Pt(4)	57.78 (3)
Ru(3)–Pt(2)–C(41)	158.4 (4)	Pt(3)–Ru(2)–Ru(3)	87.51 (4)
Pt(2)–Pt(3)–Pt(4)	59.45 (2)	Pt(4)–Ru(2)–Ru(3)	57.94 (3)
Pt(2)–Pt(3)–Ru(1)	60.87 (3)	Pt(2)–Ru(3)–Pt(4)	57.33 (3)
Pt(2)–Pt(3)–Ru(2)	93.11 (3)	Pt(2)–Ru(3)–Ru(2)	87.46 (4)
Pt(2)–Pt(3)–Ru(5)	93.75 (3)	Pt(4)–Ru(3)–Ru(2)	57.76 (3)
Pt(2)–Pt(3)–C(30)	150.5 (3)	Pt(2)–Ru(4)–Pt(4)	54.83 (3)
Pt(4)–Pt(3)–Ru(1)	95.55 (3)	Pt(2)–Ru(4)–Ru(5)	88.63 (4)
Pt(4)–Pt(3)–Ru(2)	61.40 (3)	Pt(4)–Ru(4)–Ru(5)	60.30 (3)
Pt(4)–Pt(3)–Ru(5)	65.72 (3)	Pt(3)–Ru(5)–Pt(4)	54.52 (3)
Pt(4)–Pt(3)–C(30)	147.5 (4)	Pt(3)–Ru(5)–Ru(4)	85.94 (4)
Ru(1)–Pt(3)–Ru(2)	68.55 (3)	Pt(4)–Ru(5)–Ru(4)	59.80 (4)
Ru(1)–Pt(3)–Ru(5)	154.35 (4)	Ru(1)–C(11)–O(11)	168 (1)
Ru(2)–Pt(3)–Ru(5)	112.48 (4)	Ru(3)–C(33)–O(33)	168 (1)
Pt(2)–Pt(4)–Pt(3)	61.01 (2)	Pt(2)–C(41)–O(41)	119 (1)
Pt(2)–Pt(4)–Ru(2)	93.68 (3)	Ru(4)–C(41)–O(41)	163 (1)
Pt(2)–Pt(4)–Ru(3)	61.50 (3)	Ru(4)–C(44)–O(44)	168 (2)
Pt(2)–Pt(4)–Ru(4)	59.51 (3)	Ru(5)–C(52)–O(52)	166 (1)
Pt(2)–Pt(4)–Ru(5)	91.15 (3)	Ru(5)–C(53)–O(53)	167 (1)
Pt(2)–Pt(4)–C(40)	147.5 (4)	M–C(av)–O	176 (2)

1.27 (1).[10,11] There is one strong semibridging carbonyl ligand, C(33)–O(33), bonding to the platinum atom, Pt–C(33) = 2.42 (1) Å and Ru(3)–C(33)–O(33) = 160(1)°, and one weaker semibridge, C(23)–O(23), where Pt–C(23) = 2.60 (1) Å and Ru(2)–C(23)–O(23) = 165 (1)°. The molecule contains 74 valence electrons, assuming that the μ_4-η^2-CO ligand is a four-electron donor and is thus electron precise.[13]

An ORTEP diagram of the molecular structure of **3** is shown in Figure 2. Final atomic positional parameters are listed in Table V. Selected interatomic distances and angles are listed in Tables VI and VII. The cluster consists of four platinum and five ruthenium atoms. There are only a few examples of high-nuclearity platinum–ruthenium carbonyl cluster complexes,[4,9] and this is one of the largest to date. It can be described as a combination of a Pt_3Ru_3 octahedron fused to a Pt_3Ru_2 square pyramid on the common Pt_3 face with a Pt(COD) capping group on the

---

(13) Mingos, D. M. P.; May, A. S. In *The Chemistry of Metal Cluster Complexes*; Shriver, D. F., Kaesz, H. D., Adams, R. D., Eds.; VCH Publishers: New York, 1990; Chapter 2.

Table VIII. Positional Parameters and *B*(eq) for **6**

atom	*x*	*y*	*z*	*B*(eq), Å^2
Pt(1)	0.10902 (07)	0.08875 (03)	0.58246 (08)	2.08 (5)
Pt(2)	0.30575 (07)	0.18106 (03)	0.49148 (09)	2.65 (5)
Os(1)	0.24953 (07)	0.13049 (04)	0.64580 (08)	2.40 (5)
Os(2)	0.17715 (07)	0.07486 (04)	0.79521 (08)	2.38 (5)
Os(3)	0.05521 (07)	0.07559 (04)	0.36308 (08)	2.50 (5)
Os(4)	0.18437 (07)	0.13123 (04)	0.41839 (08)	2.47 (5)
O(10)	−0.0552 (13)	0.0459 (07)	0.6593 (16)	5 (1)
O(11)	0.1207 (15)	0.1950 (08)	0.7162 (17)	7 (1)
O(12)	0.3833 (16)	0.1541 (07)	0.8387 (16)	6 (1)
O(13)	0.4046 (13)	0.0785 (07)	0.5702 (18)	5 (1)
O(21)	0.0610 (14)	0.0141 (07)	0.8896 (16)	6 (1)
O(22)	0.0562 (16)	0.1367 (07)	0.8880 (18)	6 (1)
O(23)	0.2927 (13)	0.0176 (07)	0.6636 (15)	5 (1)
O(24)	0.2954 (14)	0.0807 (09)	1.0076 (16)	8 (2)
O(31)	−0.0954 (13)	0.0174 (07)	0.3764 (17)	5 (1)
O(32)	−0.0836 (14)	0.1387 (06)	0.3767 (17)	5 (1)
O(33)	0.0709 (14)	0.0733 (09)	0.1008 (15)	7 (2)
O(34)	0.2080 (14)	0.0173 (06)	0.4042 (16)	5 (1)
O(41)	0.0486 (15)	0.1923 (07)	0.478 (02)	7 (1)
O(42)	0.3394 (14)	0.0829 (08)	0.3322 (17)	7 (1)
O(43)	0.1751 (17)	0.1602 (08)	0.1658 (15)	7 (1)
C(10)	0.0071 (18)	0.0618 (09)	0.630 (02)	2.6 (6)
C(11)	0.1664 (19)	0.1699 (10)	0.691 (02)	3.3 (6)
C(12)	0.3307 (20)	0.1476 (10)	0.764 (03)	4.3 (7)
C(13)	0.3465 (16)	0.0980 (08)	0.593 (02)	2.0 (5)
C(21)	0.1046 (18)	0.0362 (09)	0.857 (02)	2.8 (6)
C(22)	0.0992 (19)	0.1122 (10)	0.849 (02)	3.7 (6)
C(23)	0.2510 (16)	0.0392 (08)	0.7117 (19)	1.8 (5)
C(24)	0.2512 (19)	0.0761 (09)	0.930 (02)	3.8 (6)
C(31)	−0.0415 (18)	0.0376 (09)	0.371 (02)	2.4 (6)
C(32)	−0.0310 (18)	0.1164 (09)	0.371 (02)	3.0 (6)
C(33)	0.0602 (17)	0.0747 (09)	0.200 (02)	2.7 (6)
C(34)	0.1530 (19)	0.0395 (10)	0.387 (02)	3.5 (6)
C(41)	0.0985 (20)	0.1687 (10)	0.461 (02)	3.9 (7)
C(42)	0.281 (02)	0.1022 (10)	0.370 (02)	4.3 (7)
C(43)	0.1736 (19)	0.1496 (09)	0.254 (02)	3.5 (6)

Ru$_3$ face of the octahedron. The Pt–Pt distances are fairly short, 2.6327 (7)–2.6740 (8) Å, but are very similar to those found in the stacked triangulated cluster anions $[Pt_{3n}(CO)_{6n}]^{2-}$ ($n = 2$–5) that were studied by Chini and Dahl.[14] The Pt–Ru distances to the capping Pt(COD) group contain two short bonds, 2.737 (1) and 2.741 (1) Å, and one long bond, 2.911 (1) Å. A similar effect was observed among the Pt–Ru distances to the Pt(COD) capping group in **2** (see above). The Pt–Ru bonds within the Pt$_3$Ru$_3$ octahedron are similar in length, 2.719 (1)–2.749 (1) Å, while the Ru–Ru bonds are the longest, 2.913 (1)–3.065 (1) Å. The Pt–Ru bond distances in the base of the Pt$_2$Ru$_3$ square pyramid, Pt(2)–Ru(4) = 2.775 (1) Å and Pt(3)–Ru(5) = 2.795 (1) Å, are significantly shorter than those to the apex, Pt(4)–Ru(4) = 2.935 (1) Å and Pt(4)–Ru(5) = 2.949 (1) Å. This could be due to the fact that the basal platinum atoms, Pt(2) and Pt(3), have a lower coordination number than the apex atom, Pt(4). Two carbonyl ligands, one on each of the Pt–Ru bonds in the base of the square-pyramidal grouping, have adopted semibridging coordinations: Pt(2)···C(41) - 2.45 (2) Å, Ru(4)–C(41)–O(41) = 163 (1) °; Pt(3)···C(53) = 2.58 (2) Å, Ru(5)–C(53)–O(53) = 167 (1)°. Compound **3** contains a total of 124 valence electrons, which is in accord with the predictions of the skeletal electron pair theory as applied to condensed polyhedra.[13]

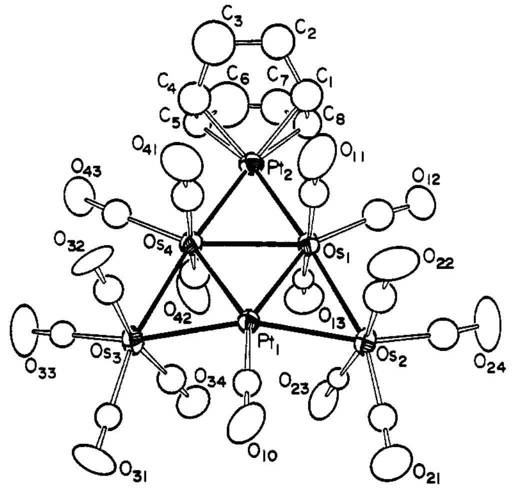

Figure 3. ORTEP diagram of Pt$_2$Os$_4$(CO)$_{15}$(COD) (**6**) showing 50% probability thermal ellipsoids.

Table IX. Intramolecular Distances (Å) for **6**

Pt(1)–Os(1)	2.662 (2)	Os(2)–C(21)	1.89 (3)
Pt(1)–Os(2)	2.701 (1)	Os(2)–C(22)	1.87 (3)
Pt(1)–Os(3)	2.697 (1)	Os(2)–C(23)	1.94 (3)
Pt(1)–Os(4)	2.673 (2)	Os(2)–C(24)	1.90 (3)
Pt(1)–C(10)	1.87 (3)	Os(3)–Os(4)	2.833 (2)
Pt(2)–Os(1)	2.674 (2)	Os(3)–C(31)	1.98 (3)
Pt(2)–Os(4)	2.668 (2)	Os(3)–C(32)	1.94 (3)
Pt(2)–C(1)	2.15 (3)	Os(3)–C(33)	1.88 (2)
Pt(2)–C(4)	2.14 (3)	Os(3)–C(34)	1.96 (3)
Pt(2)–C(5)	2.21 (3)	Os(4)–C(41)	1.91 (3)
Pt(2)–C(8)	2.19 (3)	Os(4)–C(42)	1.85 (3)
Os(1)–Os(2)	2.845 (2)	Os(4)–C(43)	2.02 (3)
Os(1)–Os(4)	2.797 (1)	C(1)–C(8)	1.37 (4)
Os(1)–C(11)	1.95 (3)	C(4)–C(5)	1.32 (4)
Os(1)–C(12)	1.92 (3)	O–C(av)	1.14 (3)
Os(1)–C(13)	1.94 (3)		

Table X. Intramolecular Bond Angles (deg) for **6**

Os(1)–Pt(1)–Os(2)	64.07 (4)	Pt(2)–Os(1)–Os(4)	58.33 (4)
Os(1)–Pt(1)–Os(3)	125.91 (5)	Os(2)–Os(1)–Os(4)	116.52 (5)
Os(1)–Pt(1)–Os(4)	63.25 (4)	Pt(1)–Os(2)–Os(1)	57.29 (4)
Os(1)–Pt(1)–C(10)	146.9 (7)	Pt(1)–Os(3)–Os(4)	57.76 (4)
Os(2)–Pt(1)–Os(3)	158.76 (6)	Pt(1)–Os(4)–Pt(2)	115.91 (5)
Os(2)–Pt(1)–Os(4)	126.45 (5)	Pt(1)–Os(4)–Os(1)	58.18 (4)
Os(3)–Pt(1)–Os(4)	63.68 (4)	Pt(1)–Os(4)–Os(3)	58.57 (4)
Os(1)–Pt(2)–Os(4)	63.15 (4)	Pt(2)–Os(4)–Os(1)	58.52 (4)
Pt(1)–Os(1)–Pt(2)	116.11 (5)	Pt(2)–Os(4)–Os(3)	174.43 (5)
Pt(1)–Os(1)–Os(2)	58.64 (4)	Os(1)–Os(4)–Os(3)	115.92 (5)
Pt(1)–Os(1)–Os(4)	58.58 (4)	M–C(av)–O	176 (3)
Pt(2)–Os(1)–Os(2)	174.75 (5)		

When Pt$_2$Os$_4$(CO)$_{18}$ (**1b**) was irradiated in the presence of COD, it was converted into the hexanuclear products Pt$_2$Os$_4$(CO)$_{17}$ (**5**) (29%) and Pt$_2$Os$_4$(CO)$_{15}$(COD) (**6**) (25%), a trace of an unknown brown compound **7**, and small amounts of the known compounds Pt$_2$Os$_4$(CO)$_{12}$(COD)$_2$[7] (**8**) (6%) and PtOs$_2$(CO)$_8$(COD)[7b] (**4**) (7%). Compounds **5**, **8**, and **4** were also obtained from the thermal reaction of **1b** with COD.[7] Compound **5** contains no COD and can be obtained in a good yield (64%) simply by irradiating **1b** in the absence of COD. The molecular formula for **5** was established by its mass spectrum, which showed the parent ion at *m*/*e* = 1628 with an isotope distribution pattern for two platinum and four osmium atoms and fragment ions corresponding to the loss of each 2–17 CO ligands. Numerous attempts to obtain crystals of **5** for a structural analysis were unsuccessful.

The formula of compound **6** suggests that it is a simple COD derivative of **5**. However, we were not able to obtain **5** by reaction with COD in the presence of UV irradiation, and only **8** was obtained from the thermal reaction of **5** with COD (97 °C). Crystals of **6** suitable for X-ray diffraction analysis were obtained, and a satisfactory structural characterization was completed. An ORTEP diagram of the molecular structure of **6** is shown in Figure 3. Final atomic positional parameters are listed in Table VIII. Selected interatomic bond distances and angles are listed in Tables IX and X. The molecule exhibits the well-known "raft" structure that was first observed by Longoni[15] for the platinum–iron cluster anions $[Pt_3Fe_3(CO)_{15}]^{n-}$ (**10**; $n = 1, 2$) and more recently by Adams[3] and Garlaschelli,[16] for $n = 0$. There is a Pt(COD)

---

(14) (a) Longoni, G.; Chini, P. *J. Am. Chem. Soc.* **1976**, *98*, 7225. (b) Calabrese, J. C.; Dahl, L. F.; Chini, P.; Longoni, G.; Martinengo, S. *J. Am. Chem. Soc.* **1974**, *96*, 2614.

(15) Longoni, G.; Manassero, M.; Sansoni, M. *J. Am. Chem. Soc.* **1980**, *102*, 7973.

Scheme I

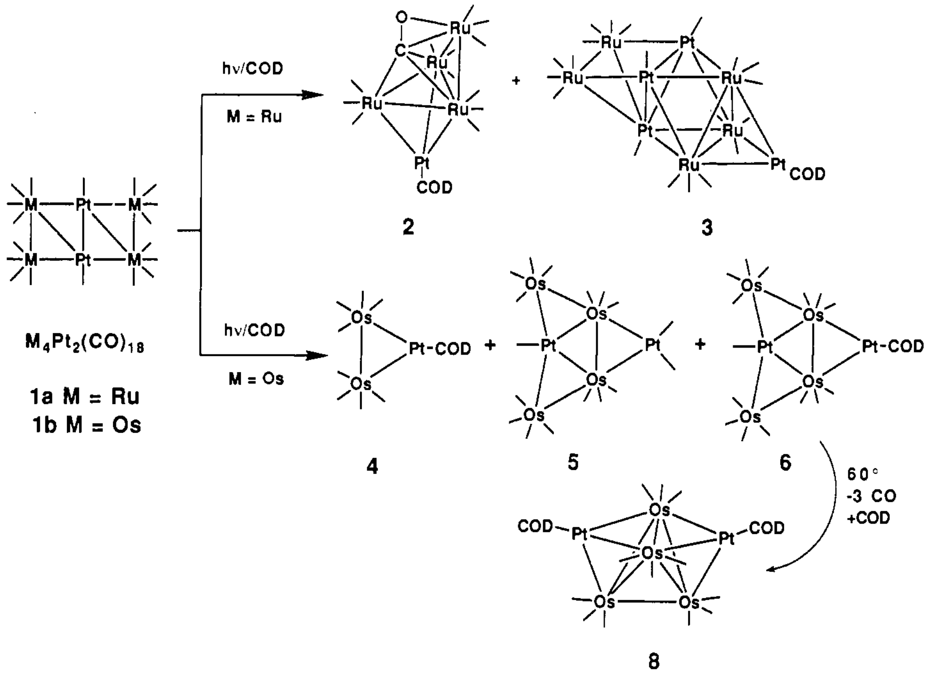

grouping in one of the outer triangles and one Pt(CO) group in the inner triangle. The hexaosmium cluster $Os_6(CO)_{17}[P(OMe)_3]_4$ (**11**)[17] exhibits a similar structure, and several other examples of cluster complexes containing the raft structure have been reported recently.[18] The osmium–osmium distances in **6** are similar to those found in **11**, Os–Os = 2.797 (1)–2.845 (2) Å. The platinum–osmium distances are slightly shorter, Pt–Os = 2.662 92)–2.701 (1) Å, but are similar to those found in the planar platinum–osmium cluster complexes $Pt_2Os_3(CO)_{14}$ (**12**)[19] and $PtOs_2(CO)_{10}$ (**9**).[6,19] Interestingly, the raft is not completely planar. The osmium atoms of the $Os(CO)_4$ groups lie on one side of the central $PtOs_2$ triangle, while the Pt atom of the Pt(COD) grouping lies on the other. The dihedral angles produced by the adjacent triangles are 170°. The COD ligand shows no unusual distortions. Its coordinated double bonds lie approximately perpendicular to the approximate plane of the raft.

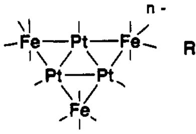
1 0

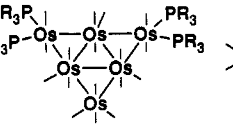
1 1

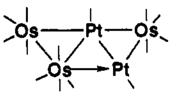
1 2

When heated to 60 °C in heptane solvent in the presence of COD, compound **6** was decarbonylated and converted to **8** in 62% yield together with very small amounts of **1b**, **4**, and **5**. UV irradiation of solutions of **6** and COD produced a similar result, but the product yields were significantly lower. Compound **6** reacted with CO at 25 °C/1 atm to yield **1b** (40%), **9**[6,19] (16%), and **5** (9%). Cyclic voltammetric measurements on compound **5** showed the presence of two reversible one-electron reduction processes at $E_{1/2}$ = −0.57 and −0.84 V, which are attributed to the formation of mono and dianionic species. The cyclic voltammogram of **5** taken in CH_2Cl_2 is shown in Figure 4. Compound **6** shows two quasireversible one-electron reductions at $E_{1/2}$ = −0.67 and −0.93 V. The larger potentials for **6** are consistent with the presence of the poorer π-acceptor ligand COD in the molecule. The poorer reversibility of the reductions in **6** might be due to greater instability of these anions also due to the presence of the poorer π-acceptor ligand COD in the molecule.

Discussion

A summary of the reactions reported in this study is shown in Scheme I. The principle products **2** and **3** obtained from the reaction of **1a** and COD in the presence of UV irradiation were clearly the result of fragmentation and reassembly of the cluster. Compound **2** has a greater ruthenium/platinum ratio than **1a**, while **3** has a greater platinum/ruthenium ratio. Compound **3** seems to be related to a series of high-nuclearity platinum–osmium carbonyl cluster complexes that we have recently obtained from the thermal decarbonylation of $Pt_2Os_3(CO)_{10}(COD)_2$[19] and $Pt_2Os_3(CO)_9(COD)_2(\mu\text{-}H)_2$.[20] The compound $Pt_4Os_6(CO)_{10}(COD)$ (**14**) is one example of these.[21] Compound **14** can be viewed as two face-shared Pt_3Os_3 octahedra with the Pt_3 face in common with a Pt(COD) capping group on one of the Os_3 triangles. The addition of a ruthenium grouping to the Pt_2Ru_2 square of **3** should produce the platinum–ruthenium analogue of **14**, and efforts to achieve this are in progress.

In contrast, the principal products obtained from the UV irradiation of **1b** in the presence of COD are the hexanuclear complexes **5** and **6**, which have the same platinum/osmium composition as **1b**. (The formation of compound **5** was independent of the presence of COD as established by a separate experiment.) The hexanuclear composition of **5** and **6** suggests

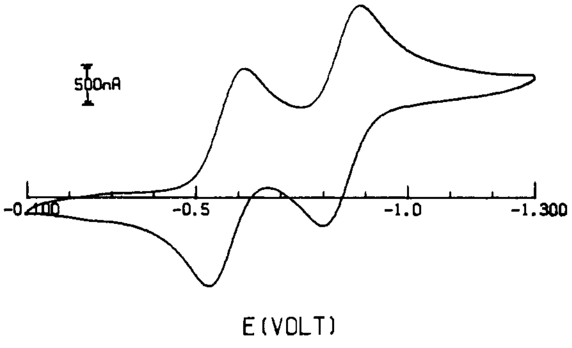

Figure 4. Cyclic voltammogram of **5** recorded in CH_2Cl_2.

---

(16) Pergola, R. D.; Garlaschelli, I.; Mealli, C.; Proserpio, D. M.; Zanello, P. *J. Cluster Sci.* **1990**, *1*, 93.

(17) Goudsmit, R. J.; Johnson, B. F. G.; Lewis, J.; Raithby, P.; Whitemire, K. H. *J. Chem. Soc., Chem. Commun.* **1982**, 640.

(18) See ref 13, Table 2.19.

(19) Adams, R. D.; Chen, G.; Lii, J. C.; Wu, *W. Inorg. Chem.* **1991**, *30*, 1007.

(20) Adams, R. D.; Lii, J. C.; Wu, W. *Inorg. Chem.* **1991**, *30*, 3613.

(21) Adams, R. D.; Lii, J. C.; Wu, W. *Inorg. Chem.* **1991**, *30*, 2257.

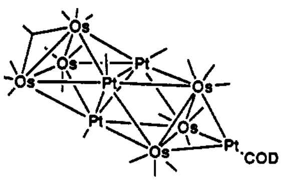

14

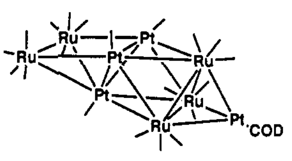

3

that cluster fragmentation is not as important a process in these reactions, although a significant amount of rearrangement of the metal-metal bonds is certainly required to transform the ladder structure of **1b** into the raft of **6**. This process is also readily reversible, since the treatment of **6** with CO at 25 °C regenerated **1b** in 40% yield in 5 min. Although the structure of **5** was not established crystallographically, it seems most likely that its structure is analogous to that of **6** with two carbonyl ligands on the platinum atom in the place of the COD ligand. The thermal decarbonylation of **6** leading to the formation of the closed-cluster complex **8** is similar to the cluster-closing transformations of $Os_6(CO)_{21}$ to $Os_6(CO)_{18}$[22,23] and $Os_5(CO)_{19}$ to $Os_5(CO)_{16}$[24] and is a natural consequence of decreased ligation.

The redox behavior of **5** and **6** is similar to that exhibited by $Pt_3Fe_3(CO)_{15}$[3,16] and a variety of phosphine and phosphite analogues of **11**.[23] The additional electrons in the anions of $[Pt_3Fe_3(CO)_{15}]^{n-}$ (n = 1,2) were proposed to occupy a low-lying in-plane antibonding orbital of A_2' symmetry that was concentrated principally on the three platinum atoms of the inner triangle.[16,25] The similar redox behavior of **5** supports its formulation as a raft type structure.

Acknowledgment. These studies were supported by the National Science Foundation under Grant No. CHE-8919786. We thank Dr. John Dawson for the use of his electrochemical equipment.

Supplementary Material Available: Tables of hydrogen atom and selected carbon atom positional parameters, anisotropic thermal parameters, and bond angles (17 pages); listings of structure factor amplitudes (56 pages). Ordering information is given on any current masthead page.

---

(22) Nicholls, J. N.; Farrar, D. H.; Jackson, P. F.; Johnson, B. F. G.; Lewis, J. *J. Chem. Soc., Dalton Trans.* **1982**, 1395.

(23) Goudsmit, R. J.; Jeffrey, J. G.; Johnson, B. F. G.; Lewis, J.; McQueen, R. C. S.; Sanders, A. J.; Liu, J.-C. *J. Chem. Soc., Chem. Commun.* **1986**, 24.

(24) Farrar, D. H.; Johnson, B. F. G.; Lewis, J.; Raithby, P.; Rosales, M. J. *J. Chem. Soc., Dalton Trans.* **1982**, 2051.

(25) Evans, D. G.; Mingos, D. M. P. *Organometallics* **1983**, *2*, 435.

Contribution from Department of Chemistry, 6-331,
Massachusetts Institute of Technology, Cambridge, Massachusetts 02139

Bimetallic Hydrazido(3– and 4–) and Nitrido Complexes of Tungsten Containing the $W(\eta^5\text{-}C_5Me_5)Me_3$ Core

Timothy E. Glassman, Andrew H. Liu, and Richard R. Schrock*

Received May 29, 1991

$Cp^*Me_3W{=}NNH_2$ (**1**) is successively deprotonated by Li-*n*-Bu to yield $[Cp^*Me_3W{=}NNHLi]_x$ (**2**) and then $[Cp^*Me_3W{=}NNLi_2]_x$ (**3**). Water reacts with **2** or **3** to re-form **1**. $SiMe_3Cl$ reacts with **2** or **3** to give $Cp^*Me_3W{=}NNH(SiMe_3)$ or $Cp^*Me_3W{=}NN(SiMe_3)_2$, respectively. Reaction of 0.5 equiv of $MgNp_2(TMEDA)$ with **1** yields $[Cp^*Me_3W{=}NNH]_2[\mu\text{-}Mg(TMEDA)]$, which can be recrystallized from THF to yield structurally characterized $[Cp^*Me_3W{=}NNH]_2[\mu\text{-}Mg(THF)_4]$ (**6**-$(THF)_4$; space group $P2_1/n$ (No. 14), a = 12.380 (6) Å, b = 15.252 (6) Å, c = 30.618 (8) Å, β = 97.91 (3)°, V = 5726 (7) Å^3, MW = 1099.14, ρ(calcd) = 1.275 g/cm^3, Z = 4, R = 0.082, R_w = 0.132). $Cp^*Me_3W{=}NNH\{MgNp(TMEDA)\}$ (**7**) is obtained upon treating **1** with 1 equiv of $MgNp_2(TMEDA)$ at –40 °C; warming **7** to room temperature yields $[Cp^*Me_3W{=}NN]_2[\mu\text{-}Mg(TMEDA)]_2$ (**8**). $Cp^*Me_3W{=}N{-}N{=}TaCp^*Me_2$ (**9**) has been prepared by treating Cp^*TaMe_3Cl with **6** or Cp^*TaMe_4 with **1**. Complexes of the type $Cp^*Me_3W{=}NNH(ZrCp_2R)$ (R = Me (**10a**), CH_2Ph (**10b**)) are the products of the reactions between **1** and Cp_2ZrR_2, but they do not readily eliminate methane or toluene to generate a hydrazido(4–) complex. **10a** and **10b** react slowly with **1** to form $[Cp^*Me_3W{=}NNH]_2ZrCp_2$ (**11**). The tantalum and zirconium complexes react readily with water to re-form **1**. Reaction of $[Cp^*Me_3W{=}NLi]_x$ (**12**) with $Cp^*WMe_3(OTf)$ yields the symmetric, mixed-valent bridging nitride $[Cp^*Me_3W]_2(\mu\text{-}N)$ (**13a**), which has been characterized crystallographically (space group $P2_1/c$ (No. 14), a = 8.390 (4) Å, b = 20.341 (6) Å, c = 8.733 (4) Å, β = 117.83 (2)°, V = 1318 (2) Å^3, MW = 742.37, ρ(calcd) = 1.870 g/cm^3, Z = 2, R = 0.057, R_w = 0.063). The geometry about the tungsten in **13a** is square pyramidal, a center of inversion defines a linear W–N–W backbone that has a W–N distance of 1.8475 (8) Å. **13a** can be oxidized to yield $\{[Cp^*Me_3W]_2(\mu\text{-}N)\}^+$ (**13b**). **12** also reacts with Cp^*TaMe_3X (X = Cl, OTf) or $Cp^*TaMe_2(OTf)_2$ to give the unsymmetrical "metalloimido" complex $Cp^*Me_3W{\equiv}N\text{-}TaCp^*Me_3$ (**15**) or the bridging nitride $Cp^*Me_3W{=}N{=}TaCp^*Me_2(OTf)$ (**14**), respectively.

Introduction

Dinitrogen is activated by a variety of early transition metals (e.g., those in $Ti(OEt)_4$, $(\eta^5\text{-}C_5H_5)_2ZrCl_2$, $VCl_3(THF)_3$, and WCl_6) that have been reduced by sodium, lithium, magnesium, metal hydrides, or metal alkyls.[1] Mechanisms have been proposed that involve lithiated or magnesiated hydrazido and imido intermediates specifically.[2,3] Proposals for the activation of dinitrogen that involve two or more transition-metal centers are also common.[4-6] Typical multimetallic hydrazido species that have been proposed include trimetallic hydrazido(4–) derivatives (A), bimetallic hydrazido(3–) derivatives (B), and bimetallic hydrazido(4–) derivatives (C). Once the N–N bond has been cleaved, species that contain only one nitrogen atom bound between two or more metals (e.g., bridging nitrides, metalloimides, etc.) are proposed to be formed in such systems.

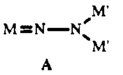

$M{=}N{-}N(M')_2$

A

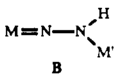

$M{=}N{-}N(H)(M')$

B

$M{=}N{-}N{=}M'$

C

We have been exploring the role of relatively high oxidation state (d^0–d^2) complexes in activating and reducing molecular nitrogen. Most recently, several hydrazido(4–) derivatives of the

---

(1) *New Trends in the Chemistry of Nitrogen Fixation*; Chatt, J., da Camara Pina, L. M., Richards, R. L., Eds.; Academic Press: New York, 1980.

(2) Shilov, A. E. *Russ. Chem. Rev.* (*Engl. Transl.*) **1974**, *43*, 378 and references therein.

(3) Yamamoto, A.; Miura, Y.; Ito, T.; Chen, H.-L.; Iri, K.; Ozawa, F.; Miki, K.; Sei, T.; Tanaka, N.; Kasai, N. *Organometallics* **1983**, *2*, 1429.

(4) Chatt, J.; Dilworth, J. R.; Richards, R. L. *Chem. Rev.* **1978**, *78*, 589 and references therein.

(5) Leigh, G. J. *J. Mol. Catal.* **1988**, *47*, 363.

(6) Leigh, G. J. *Transition Met. Chem.* (*London*) **1986**, *11*, 118.